91602
new 82-10

LEGAL NOTICE

This report was prepared by Ontario Hydro and, while effort has been made to assure the accuracy and applicability of the material contained herein, neither Ontario Hydro nor any person acting on its behalf:

(a) makes any warranty, express or implied with respect to the use of any information, apparatus, method or process disclosed in this report or that such use may not infringe privately owned rights; or

(b) assumes any liability with respect to the use of, or for damages resulting from the use of, any information, apparatus, method or process disclosed in this report.

ontario hydro
research division

COMPLIMENTARY COPY
Please Credit Ontario Hydro Research if Reproduced in Whole or in Part

LASER-BASED SEPARATION OF ZIRCONIUM ISOTOPES

Research Report No 87-322-K

Hugh D. Morrison
Physicist
Science Section
Electrical Research Department

ABSTRACT

This report describes a new scheme for depleting zirconium-91 in zirconium based on the atomic vapour laser isotope separation (AVLIS) method. Prospects and future directions in zirconium AVLIS are discussed.

job	file	date	report no.
16-529	819.39	January 11, 1988	87-322-K

91602
new 82-10

ontario hydro
research division

To: Dr. D. Mills
Director of Research

LASER-BASED SEPARATION OF ZIRCONIUM ISOTOPES

A recent report presented arguments in favour of separating zirconium isotopes and discussed a laser-based method for doing so /1/. The main argument is that reducing the concentration of one isotope, zirconium-91, reduces significantly the neutron absorption cross-section of zirconium. This effect is of great interest to the nuclear power industry because zirconium is the major element in the core components of nuclear reactors. Lower neutron absorption in reactor components would provide greater flexibility in the design of nuclear reactors. For example, if the concentration of zirconium-91 were reduced by half, from 11% in natural abundance to 6.5%, then reactor components could be made 50% thicker without increasing neutron absorption.

The laser-based method for zirconium isotope separation is known as atomic vapour laser isotope separation (AVLIS). In this technique, laser light selectively ionizes the zirconium-91 in a beam of neutral zirconium atoms. Physical separation of the ions from the neutral atoms is then accomplished in a relatively simple manner using electrically charged plates. The previous report /1/ discussed the laser part of AVLIS based on experimental measurements of the spectroscopy of light absorption by atomic zirconium. The experiments were carried out in the laboratories of the Laser Chemistry Group in the National Research Council of Canada. The spectroscopy revealed the type of laser required and some of the necessary conditions for efficient isotope separation. The results also demonstrated the need for more detailed measurements of the light absorption pathways to ionization, known as photoionization, in zirconium. Thus, a second set of experiments was performed at NRC. The results of all the experiments are described in a paper submitted for publication in Applied Physics B and attached here as an Appendix.

job	file	date	report no.
16-529	819.39	January 11, 1988	87-322-K

The paper identifies a considerable improvement in proposed schemes for depletion of zirconium-91 based on AVLIS. The problem has been to find a method that could photoionize most of the zirconium-91 without also photoionizing most of the other isotopes. A previous scheme /2/ successfully demonstrated isotope separation, but could only access a small fraction of the zirconium-91. The new scheme accesses almost all of the zirconium-91 by exploiting a distinctive feature of its spectroscopy only revealed at high resolution. In particular, the paper discusses several pathways to photoionization that exhibit this feature, and demonstrates isotope depletion achieved on one of these pathways with a new laser specially constructed for the task. Thus, the many technical results in the paper represent a significant advance along the route to developing AVLIS for zirconium.

One reason for pursuing AVLIS, as opposed to non-laser methods, is the advanced state of development of AVLIS technology for uranium enrichment in many parts of the world but most noticeably in the United States of America /3/. There are many parallels between AVLIS for uranium and AVLIS for zirconium. The technologies employed in uranium AVLIS are applicable to zirconium AVLIS in general but differ in detail. Thus, the commercial development of uranium AVLIS bodes well for the prospect of successfully developing zirconium AVLIS.

In conclusion, the attached paper provides encouragement for the development of zirconium AVLIS. Future studies of zirconium AVLIS should be directed at refining our knowledge of the photoionization process to select the best pathway. The other two processes in AVLIS, generating the atomic beam and collecting the ions separately from the atoms, also need to be examined in detail.

Approved:

A.F. Baljet
Manager
Electrical Research Department

Submitted:

H.D. Morrison
Physicist
Science Section
Electrical Research Department

REFERENCES

1. H.D. Morrison, "Photoionization schemes for atomic vapour laser isotope separation of zirconium," Research Report 87-60-K.

2. M.R. Humphries, O.L. Bourne and P.A. Hackett, "Laser isotope separation of zirconium atoms cooled in a supersonic beam," Chem. Phys. Lett. 118, 134-139 (1985).

3. J.L. Emmett, W.F. Krupke and J.I. Davis, "Laser R&D at the Lawrence Livermore National Laboratory for fusion and isotope separation applications," IEEE J. Quantum Electron. QE-20, 591-602 (1984).

APPENDIX

Pulsed Single Mode Laser Ionization of Hyperfine Levels of Zirconium-91

(Submitted to Applied Physics B)

Pulsed Single Mode Laser Ionization of Hyperfine Levels of Zirconium-91.‡

P.A. Hackett, H.D.Morrison,* O.L. Bourne, B. Simard and D.M. Rayner

Laser Chemistry Group

Division of Chemistry

National Research Council of Canada

Ottawa, Ontario, Canada K1A 0R6

‡Issued as NRC No. 28183

*NRC Guest Scientist, Summer 1986, permanent address Ontario Hydro Research Division, 800 Kipling Avenue, Toronto, Ontario, Canada, M8Z 5S4.

87-322

ABSTRACT.

This paper identifies a considerable improvement in proposed schemes for isotopic depletion of zirconium-91 based upon the Atomic Vapour Laser Isotope Separation method (AVLIS). High resolution laser induced fluorescence spectroscopy of atomic beams of zirconium produced via laser vaporization/ supersonic expansion has been used to identify transitions of zirconium with suitable hyperfine structure. Casimir magnetic dipole and electric quadrupole coupling constants and isotope shifts have been derived and are reported herein for 5 excited configurations. Transitions which allow selective excitation of zirconium-91 while at the same time allowing a single frequency laser to interact with all hyperfine split levels of the ground state have been identified. Isotope enrichment has been demonstrated on one such transition ($z^3F_3^0 \leftarrow a^3F_2$ at 593.7 nm) using a specially constructed pulsed, single longitudinal mode dye laser oscillator. Suitable intermediate levels in a multi-step resonance ionization pathway have been identified by two color resonance ionization spectroscopy. Prospects and future directions in zirconium AVLIS are discussed.

PACS: 82.50. Et, 35.10.Fk, 32.

INTRODUCTION.

Zirconium metal is vital to the nuclear power industry because of its low cross-section for thermal neutron absorption. This property combined with its good metallurgical properties makes zirconium almost ideal for nuclear reactor core components such as pressure tubes and calandria and for the cladding of nuclear fuel bundles. Zirconium alloys are used exclusively for these components in CANDU reactors (Canadian Deuterium Uranium). However, reactor operation could be improved if the thermal neutron absorption cross-section of zirconium in reactor components were reduced further. Of particular interest is the possibility of increasing the thickness of pressure tubes to extend their service lifetimes without increasing, but perhaps decreasing, their neutron absorption. It has been recognized for many years that depleting or removing entirely one of the isotopes of zirconium would reduce its neutron cross-section. Zirconium has five isotopes of atomic mass 90, 91, 92, 94 and 96. The mass 91 isotope has a natural abundance just over 11%, but it accounts for 75% of the thermal neutron absorption cross-section in natural zirconium. By reducing the concentration of ^{91}Zr to 3% the neutron cross-section of the denatured zirconium would be less than half that of the natural metal. The pressure tubes in modern CANDU reactors are constructed with the Zr-2.5 Nb alloy, zirconium 2.5% niobium. Denaturing the zirconium in this alloy to the same extent would reduce the neutron cross-section by 45%, and would allow for an 80% increase in pressure tube thickness without increasing neutron absorption. The use of zirconium containing only 3% ^{91}Zr for all in-core components would provide greater flexibility in the design of nuclear reactors and that could result in longer service lifetimes, improved neutron economy and extended fuel cycles.

One of the methods that has been demonstrated to separate zirconium isotopes is atomic vapour laser isotope separation (AVLIS) performed with laser pumped tunable dye lasers. This method is particularly attractive in view of the advanced state of development of AVLIS technology for uranium enrichment in many parts of the world but most noticeably in the United States of America [1]. There are many parallels between AVLIS of zirconium and AVLIS of uranium. Both elements are very refractory with highly reactive liquid and vapour phases. Both elements have atomic transitions across the visible region of the spectrum and both have similar ionization potentials. The most significant difference in the optical spectroscopic properties of these elements, as it affects AVLIS technology at least, is that for uranium there is a large specific isotope shift. Zirconium lies near the middle of the periodic table, N=40, where both the nuclear mass and volume effects on the isotope shift are small. It was pointed out in the first laboratory demonstration of zirconium AVLIS that this did not preclude selective removal of zirconium-91 by AVLIS technology [2]. This is because all even-neutron number even-proton number isotopes have zero nuclear spin. Thus hyperfine splitting on the zirconium-91 nucleus results in the convenient situation that the optical transitions of zirconium-91 are generally split away from the clump of transitions of the remaining four isotopes at the centre of the spectral line. It seems therefore that AVLIS of zirconium-91 based upon hyperfine split transitions may not be technically infeasible. There is however a significant problem with this approach as demonstrated and commented upon in our earlier paper [2]. In that paper, selective ionization of all isotopes was demonstrated based upon selective absorption of a photon on the $z^3F_2^0 \leftarrow a^3F_2$ transition, followed by an ionizing photon at 308 nm. Although hyperfine splitting allows selective

ionization of zirconium-91 it has its deleterious consequences. For the particular transition studied the splitting in the upper state was negligible [3] in comparison with the reasonably large splitting observed in the ground state [4]. The consequence of this for AVLIS is that only one hyperfine level of the ground level of zirconium-91 could be accessed at any one selective laser frequency. As the nuclear-spin of zirconium-91 is 5/2 the $^3F_2$ ground state is split into five hyperfine levels (F"=1/2, 3/2, 5/2, 7/2, 9/2). In principle then, five high resolution dye lasers would be required to deplete all zirconium-91 from an atomic beam source. In practice there will be population on the two low lying spin-orbit excited levels and a further twelve hyperfine levels could be involved.

We have undertaken the present work, which is a further investigation of the spectroscopy of zirconium vapour, in order to improve upon this position. We were motivated to investigate the hyperfine structure of other low lying levels of zirconium atoms to ascertain if the spectroscopic situation described above was general or whether we could identify transitions in which one could interact with multiple hyperfine levels of the ground state at single laser frequencies in an isotopically selective way. Thus, the high resolution spectroscopy carried out here was primarily for the purpose of pattern determination and recognition rather than for the determination of excited state hyperfine parameters in their own right.

As a consequence of the work reported here, we have identified transitions in the optical spectrum of zirconium which have the property that all (or the majority) of lower state hyperfine levels of zirconium-91 may be excited by a single laser of moderate frequency width (≈300 MHz) while at the same time these transitions are removed from the transitions of even isotopes.

Finally, we have shown that these newly identified levels are suitable for zirconium AVLIS by carrying out two-color resonance ionization mass spectroscopy. In these ionization studies, the first laser-photon was obtained from a simple, pulsed single longitudinal mode laser oscillator based upon Littman's design [5]. This laser was shown to have a linewidth of 500 MHz, ideally suited to the spectroscopic requirements for effective zirconium AVLIS.

EXPERIMENTAL TECHNIQUES

As in our two previous publications on the high resolution fluorescence [3] and ionization spectroscopy [2] of zirconium we have made use of atomic beams of zirconium formed via pulsed laser evaporation of solid metal targets placed before a supersonic helium expansion. Details of the atomic beam source have been given in the earlier publications and will not be repeated here [2,3]. It is sufficient to note that 15 mJ pulses from a xenon chloride excimer laser were used to produce a supersonic beam of zirconium atoms entrained in helium. The zirconium atoms were distributed over the three lowest levels with an effective electronic temperature in the range of 850K.

Low resolution fluorescence spectroscopy was carried out 10 cm down beam from the point of supersonic expansion. Zirconium atoms were viewed in fluorescence excited using an excimer laser pumped dye laser (Lumonics Hyperdye-300). The wavelengths of observed resonant transitions were verified using a Candela LS1 laser spectrometer accurate to ± 0.01 nm.

High resolution fluorescence excitation spectroscopy was carried out 65 cm from the point of supersonic expansion using the molecular beam fluorescence spectrometer previously described [3]. The fluorescence was imaged at a magnification of 5 at a 0.8 mm slit. This arrangement gave an

observed spectral width of approximately 20 MHz. Two argon ion laser pumped ring dye lasers were used throughout this work (Spectra Physics 380 D or Coherent model 699-29 operated in the autoscan mode). The wavelengths of these lasers were checked using either a Burleigh wavemeter or the Coherent Autoscan wavemeter calibrated by comparison with known fluorescence lines of iodine. No external high resolution etalon was available to assess the linearity of wavelength scans. Instead we have used the known splittings of ground state hyperfine lines as internal frequency difference standards in deriving hyperfine constants, vide infra.

Two color, resonance-enhanced ionization spectra were obtained using the molecular beam time-of-flight mass spectrometer (TOFMS) described previously [2]. In these low resolution experiments the ionization signal was integrated and no isotopic details were obtained. Two dye lasers pumped by a single Lumonics excimer laser operated on xenon chloride mix were employed. The first (Hyperdye-300) was tuned to known transitions of the three spin-orbit split levels of the ground configuration of zirconium and crossed the intersection of the axes of the atomic beam and the TOFMS so that all three were mutually orthogonal. The second (Lumonics EPD 300) laser counter-propagated through the same region after a delay (optical) of 20 ns. Both lasers were plane polarized along the TOFMS axis and no attempt was made to vary this. Neither laser was focussed, pulse energies were in the range 0.1-0.5 mJ and the beam diameters in the TOFMS interaction region were of the order of 5 mm.

In experiments designed to identify intermediate resonances the ionization signal was recorded as a function of the wavelength of the second laser. The wavelength of all resonances was established using the laser

spectrometer mentioned above. Each resonance was checked to verify that both laser beams were required to obtain ionization.

High resolution resonance ionization spectra were obtained using a specially constructed pulsed single longitudinal mode (SLM) laser tuned to the transition $z^3F_3^0 \leftarrow a^3F_2$ at 593.7 nm to provide the first photon [6]. This SLM laser was pumped by a separate xenon chloride laser and crossed the TOFMS along the path traversed by the first laser in the low resolution experiments described above. The second dye laser was as described above and was tuned to the intermediate resonance at 544.5 nm identified in the low resolution experiments. The low resolution dye laser pulse arrived 50 ns after the SLM laser pulse. The delay time was determined electronically.

The output of the TOFMS channeltron ion detector was digitized in a wide bandwidth (Tektronix 7912 AD) digitizer, signal averaged and then stored in an LSI-11 computer. In this way isotopically resolved (mass resolution ≈200) mass spectra could be obtained. Mass spectra were acquired as a function of the SLM lasing wavelength. These mass spectra were then used to determine the optical spectra of individual isotopes and the wavelength dependence of the isotopic selectivity, $^{91}\alpha$, for excitation of zirconium-91,

$$^{91}\alpha = \frac{\{^{91}I/(\Sigma I - ^{91}I)\}_{\lambda}}{\{^{91}f/(1-^{91}f)\}_{natural}}$$

where ^{91}I and $\Sigma\ I$ represent the ionization intensity for zirconium-91 and all isotopes of zirconium respectively, determined at wavelength λ. The fractional natural abundance of zirconium-91 is represented as ^{91}f. It was verified in mass-resolved, low (optical) resolution experiments i.e. non-SLM excitation, that ^{91}f was 0.11 and that $^{91}\alpha$ was ≈1.00.

The wavelength of the SLM laser was varied by pressure tuning using nitrogen gas, vide infra. In these experiments the conversion from nitrogen pressure change to change in wavelength was simplified by comparison of the even isotope ionization peaks with the isotope shifts for the $z^3F_3^0 \leftarrow a^3F_2$ transition determined in this work.

The pulsed single longitudinal mode dye laser was built specifically for these experiments according to Littman's design [5]. This design is based upon a short cavity length which ensures a reasonably wide spacing of cavity modes. A grazing incidence diffraction grating then has sufficient resolving power to ensure lasing on a single longitudinal mode. Advantages of SLM operation of excimer pumped pulsed dye lasers are smooth temporal (gaussian) pulse shapes i.e. no mode beating and narrow frequency width. Littman demonstrated frequency widths (FWHM) of ≈200 MHz in his original work, this using optics flat to $\lambda/40$ [5]. Our laser used $\lambda/10$ optics and our frequency widths were found to be 500 MHz, vide infra.

A difficulty with Littman's design is associated with reproducible fine tuning. This is a consequence of the use of mechanical tuning mechanisms which are notoriously subject to stick-slip and hysteresis problems. We have approached this problem by pressure tuning the dye laser [7]. For the small frequency difference required in this work this is an ideal solution but for larger frequency scans there is a significant problem due to mode mismatching. This is a consequence of the fact that changing the cavity pressure does not change the refractive index (effective length) of the dye cell optics nor of the dye solution. Inevitably tuning the laser frequency over a wide enough range will destroy the SLM condition and two adjacent cavity modes will compete. We have avoided this by adding a small, over pressurized, slave

chamber to the cavity. Pressure changes in the cavity (neighbourhood of the grating) serve to change the laser frequency, pressure changes in the slave chamber serve to maintain single mode operation by changing the cavity length. The construction and operation of this pressure-tuned, SLM laser are fully described elsewhere [6].

In the present study the SLM oscillator was operated at an output pulse energy of 0.2 μJ. This pulse was amplified by a factor of 20 in a standard rectangular dye cell pumped by 3 mJ of 308 nm radiation. The laser was tuned with pure nitrogen gas. The tuning rate was found to be 140 MHz per Torr.

RESULTS AND DISCUSSION.

To demonstrate an improved method of atomic vapour laser isotope separation (AVLIS) for zirconium, we conducted a series of four experiments. The combined results of the first three experiments identify candidate schemes for multi-step resonant photoionization, the laser process in AVLIS. Measurements from the fourth experiment illustrate the advantages of the single longitudinal mode dye laser for selective excitation of ^{91}Zr.

The search for photoionization schemes begins by considering a few practical aspects of AVLIS as applied to zirconium. Consider first that the ionization potential of zirconium lies 53506.0 cm^{-1} above the ground state term a^3F_2 [8]. Photoionization can be achieved by the resonant absorption of three photons with an average wavelength of 560 nm. Tunable energy in the range from 530 nm to the infrared is available from copper laser pumped dye lasers, a laser system well suited to the requirements of AVLIS [1]. Therefore, we assume that any scheme for photoionizing zirconium must consist of three resonant steps at wavelengths generated by copper laser pumped dye lasers. Given the

great number of transitions in zirconium, the assumption is not too restrictive.

Two factors in the photoionization scheme directly affect the economics of AVLIS. One factor is the amount of laser energy required to provide a given separation of zirconium isotopes. To minimize the total laser energy required, we minimize the laser energy expended on non-selective excitation. Thus, we assume that all the isotopic selectivity occurs in the first excitation step of a multi-step scheme. The second factor is the fraction of zirconium atoms available for photoionization. Previous fluorescence measurements on a zirconium atomic beam have indicated that three electronic states are populated, the ground state and two metastable states at 570 cm^{-1} and 1241 cm^{-1}. At least the lower two states, preferably all three, should be accessed in the first excitation step for maximum process efficiency. This could make a photoionization scheme very complex. However, the number of different wavelengths in a complete scheme is minimized if we assume that all first step transitions have a common excited level.

Table I lists the "allowed" transitions to all the excited levels in zirconium that are accessible from at least the lower two electronic states by copper laser pumped dye lasers. Transitions not allowed by Russell-Saunders coupling have been neglected. The first set of experiments examined laser induced fluorescence at low resolution on most of the transitions listed in Table I. These experiments verified the transition wavelengths and established their isolation from nearby transitions. Then, we probed five of the first step transitions with laser induced fluorescence at high resolution to measure the isotope and hyperfine shifts of the four excited levels listed in Table 1. In the third set of experiments, resonant second steps from the first excited

levels were discovered by two color resonance ionization. The fourth and final experiment employed the single longitudinal model dye laser in single resonance ionization. This experiment measured the selectivity for photoionizing ^{91}Zr by the simultaneous excitation of all its hyperfine levels in a first step transition.

Low Resolution Laser Induced Fluorescence

Eight of the ten transitions listed in Table I have been scanned by laser induced fluorescence at low resolution (0.05 cm^{-1}). The two exceptions are the transitions at 635.9 and 640.9 nm. At this resolution the shifts of the even isotopes and the hyperfine shifts of ^{91}Zr are not apparent. The scans show no interfering transitions within 1 cm^{-1} of the transitions examined. The relative fluorescence intensities provide qualitative confirmation of the relative transition linestrengths predicted by Russell-Saunders coupling. To improve the estimates of the relative linestrengths, the variation in dye laser intensity with wavelength must be considered. Direct comparison is possible, however, in cases where the transitions are closely spaced in wavelength and laser intensity variations are neglible. For example, the electronic temperature of the atomic beam was estimated as ~850 K by Humphries et al. [2] from the intensities of the transitions $z^3F_J^0 \rightarrow a^3F_J$ where J=2,3 and 4. These transitions are spaced only 2 nm apart. Now consider the three transitions to the $z^3D_3^0$ level. The greatest fluorescence intensity was observed on the 588 nm transition, and the least intensity on the 548 nm transition. Russell-Saunders coupling predicts relative linestrengths of 0.2:8.8:100 for these transitions in order of increasing wavelength. Correcting for a Boltzman population distribution with a temperature of 850 K changes those ratios to 0.9:21.4:100, which agrees qualitatively with the observed ratios of intensity. The range of

linestrengths for transitions to the $z^3D_3^0$ level is the widest range of the four excited state levels listed in Table I. The relative linestrengths of the first step transitions will have to be considered when selecting a complete photoionization scheme.

High Resolution Laser Induced Fluorescence

To resolve the features of the isotope shifts and hyperfine structure in zirconium, the narrow linewidth of a ring dye laser was employed in laser induced fluorescence. The five transitions listed in Table 1 that lie between 579 and 615 nm were scanned with a resolution of ~20 MHz. Prior assignment of the peaks in the 613 nm spectrum [3], shown in Fig. 1, simplified the analysis of the other spectra (for example see Fig. 2). In each spectrum, four central peaks spanning ~500 MHz were indentified as the even isotopes with peak heights proportional to their natural abundances. All other peaks were attributed to hyperfine transitions in ^{91}Zr. Identifying the quantum numbers of the hyperfine transitions was based on: (a) relative intensities with respect to the Russell-Saunders coupling linestrengths [9]; and (b) pattern recognition by comparison with spectra predicted from zero-field energy splittings. The splittings in both the upper and lower states are calculated from the Casimir magnetic dipole (A) and electric quadrupole (B) constants [9]. The A and B constants for all three lower states are known from atomic beam magnetic resonance [4]. The hyperfine peaks in the 613 nm spectra had been assigned by assuming that A and B were both zero in the upper state [3]. A better estimate of A is -5.7±1.0 MHz, obtained from the splitting of the highest frequency doublet peak, the (9/2, 7/2) → 9/2 transitions.

The frequency tuning rates for all the scans at 613, 593, 614 and 579 nm were not calibrated with an etalon. However, as the lower state A and B

hyperfine constants were well known, each scan provided a self-calibration once the hyperfine transitions were identified. Thus, for each scan at these wavelengths, a least-squares fit was applied to a set of equations, one equation for each hyperfine transition. Each equation related the observed spacing between the hyperfine peak and the ^{90}Zr peak to the known hyperfine energy splitting in the lower state and to a set of four parameters (see Fig. 3). The parameters were A and B for the upper state, the isotope shift of the hypothetical non-split ^{91}Zr line with respect to the ^{90}Zr line, and the scaling factor of the scan to convert measured spacings to MHz. Thus, the least-squares fit provided best values for these four parameters. The even isotope shifts were calculated from the observed shifts with the scaling factors. The entries for A, B and the isotope shifts in Tables II and III for the first four transitions were obtained by averaging results from several scans, and the error limits are the standard errors of the sample means.

The high-resolution scans of the 588 nm transition were calibrated with an etalon. Thus, the positions of the hyperfine peaks with respect to ^{90}Zr were measured for each scan and then combined into one set of values for the least-squares fit. The small standard deviation listed for A and B in this case is a direct result of the limited data set employed and not a reflection of an improved measurement technique. While we have reported the standard deviation of the fit, the true error limits are probably consistent with the other entries in Table II.

The isotope shifts [10] and hyperfine structures [11] for these and several other transitions of atomic zirconium have recently been reported. The techniques of intermodulated saturated optogalvanic spectroscopy and polarization intermodulated excitation spectroscopy (POLINEX) were used in both

studies. As a general comparison of the work carried out by Chevalier et al. and that reported here we note that their absolute frequency difference scale is considerably more accurate, a consequence of their use of an external Koster interferometer with a 187 MHz fringe spacing; whereas, our spectra are generally of smaller linewidth and greater signal to noise, a consequence of the inherently low doppler width of our atomic beam method, and the complete absence of the broad background signal due to velocity changing collisions often observed in saturated two photon experiments. The derived hyperfine constants and isotope shifts are in generally good agreement, within the combined error limits of the measurements and usually within the error of the least accurate measurement. This agreement supports the assignment and analysis of the hyperfine structure proposed by both groups and in particular the rather indirect frequency difference calibration scheme used in the present work.

The implications of the measured values for the atomic structure of zirconium, in particular the presence of a marked odd-even staggering around the magic (N=50) neutron shell, have been discussed by Chevalier et al. and will not be repeated here [10]. What is of importance in the present context is the pattern of hyperfine structure present for particular transitions. The Casimir constants reported in Table II can be used to reconstruct the spectra studied in this work and to predict the spectra of transitions between the configurations listed in Table I but not studied herein. We particularly wish to identify transitions which have the property that a transition from each hyperfine level of the lower state may be excited by a single relatively narrow (~300 MHz) laser frequency while at the same time requiring that the frequency for the zirconium-91 "clump" be removed from the frequency of the even isotope

"clump". The transition $z^3F_3^0 \leftarrow a^3F_2$ at 593.7 nm, shown in Fig. 2, nicely illustrates this requirement. The transitions (F' ← F") 7/2 ← 9/2, 5/2 ← 7/2, 3/2 ← 5/2, 1/2 ← 3/2 and 1/2 ← 1/2 lie within 300 MHz of each other and ≈1GHz from the even isotope absorption. Other transitions which we have found to have this property to a greater or lesser degree are $z^3D_2^0 \leftarrow a^3F_2$ at 561.4 nm $z^3F_3^0 \leftarrow a^3F_3$ at 614.5 nm, $z^3F_3^0 \leftarrow a^3F_4$ at 640.9 nm and the transitions to $z^3D_3^0$ given in Table I. These transitions have clearly superior characteristics for zirconium-91 AVLIS over the transition $z^3F_2^0 \leftarrow a^3F_2$ studied in earlier work [2].

Two Color Ionization.

The search for resonant second steps in potential photoionization schemes was carried out with two colour ionization. In this method atoms were excited via a ground state transition and then ionized by the absorption of two photons from a tunable laser. Peaks in the ionization spectrum arise from resonant energy levels lying between the first excited level and the ionization potential. Figure 4 illustrates the energy levels discovered from resonances above three of the four excited levels listed in Table I. No search was conducted from $z^3F_2^0$ because of the restricted range of wavelengths it allows. The two photon ionization limit from this level is 537.5 nm, just above the shortest wavelength available from a copper laser pumped dye laser.

A scan from 500 to 550 nm above the $z^3F_3^0$ level revealed only two resonances, at 35209.4±0.4 and 36067.8±0.4 cm^{-1}. The transition at 544.50 nm lies just below the two photon ionization limit of 545.5 nm. Thus, it could also serve as the ionizing step in a photoionization scheme without the necessity of a third wavelength. A 544.50 nm photon from the level at 35209.4 cm^{-1} provides an energy excess of only 69 cm^{-1} above the ionization potential.

The second resonance at 520.19 nm is much stronger, but the wavelength is too short to be provided by a copper laser pumped dye laser.

The scan for levels above $z^3D_2^0$ produced only two resonances between 545 and 560 nm. The weaker one, at 552.76 nm, corresponds to an energy level at 35904.8±0.4 cm^{-1}. The stronger transition, at 547.80 nm, corresponds to an energy level of 36068.3±4 cm^{-1}. We identify this level with the resonance 520.19 nm above $z^3F_3^0$. By the rules for Russell-Saunders coupling, the term of this level must be either $^3D_2$, $^3D_3$, $^3F_2$, or $^3F_3$. Thus, it must also be accessible from $z^3D_3^0$.

We verified this prediction in a scan from 530 to 570 nm above $z^3D_3^0$ that revealed eight resonances: 533.655, 533.917, 535.550, 552.461, 552.860, 561.022, 566.235 and 567.656 nm. The resonance at 561.022 nm corresponds to an energy level of 36067.9±0.4 cm^{-1}. Thus, this level provides a resonant step from all three of the first excited levels examined here, and is undoubtedly accessible from $z^3F_2^0$ as well. The resonance at 566.235 nm above $z^3D_3^0$ yields an energy level of 35903.8±0.4 cm^{-1}, which lies within 1 cm^{-1} of the other resonance found above $z^3D_2^0$. If we identify these two levels as one and the same, then we can assign it the term value $^3P_2$ because it was not observed as a resonance above $z^3F_3^0$. Therefore, six of the total twelve resonances discovered are attributed to only three energy levels. The optimum wavelength for ionization from these levels, as the final step in a photoionization scheme, should lie below the values indicated in Fig. 4.

One other resonance of interest is the one at 567.656 nm to a level of 35859.6±0.4 cm^{-1}. This energy lies within 1 cm^{-1} of the $(4d^25s6s)e^5F_4$ level listed by Moore [12]. A transition to this term value from $z^3D_3^0$ is forbidden by Russell-Saunders coupling, but may occur. It is also interesting to note

that 567.656 nm lies below the two photon ionization limit of 567.2 nm, and produces two photon ionization 30 cm^{-1} below the ionization potential. This observation is not at all unreasonable and may be attributed to field ionization of high lying valence or Rydberg levels close to the ionization limit. In a recent report on the determination of an accurate value of the first ionization potential it was observed that states up to 40 cm^{-1} below the first ionization limit were efficiently ionized in electric fields of only 100V/cm [8]. The field across the interaction region of the TOFMS was ≈200 V/cm in these experiments.

Isotope Separation Using The Pulsed SLM Dye Laser

The upper panel of figure 5 shows a time-of-flight mass spectrum obtained following two color resonance ionization through the $z^3F_3^0 \leftarrow a^3F_2$ transition at 593.7 nm. This spectrum was obtained using broadband, non-SLM, dye laser excitation. The lower panel of the figure shows a spectrum obtained using the SLM laser tuned to the center frequency of the transition. Clearly selective excitation of zirconium-90 has been achieved.

The dependence of $^{91}\alpha$ on the SLM laser frequency is detailed in figure 6. This figure shows the dependence of $^{91}\alpha$ on the laser frequency together with the frequency spectrum for ionization of the zirconium-90 isotope. The lower panel gives a stick representation of the structure of this transition on the same frequency scale. The frequency scale was calibrated by comparing the frequencies of even isotope ionization peaks. Several points are worthy of note. The frequency width of the zirconium-90 peak shown in figure 6 and of other even isotopes implies a laser bandwidth of ≈500 MHz. At this bandwidth selective ionization of zirconium-91 is clearly possible. Moreover this bandwidth is clearly large enough to excite multiple lower hyperfine

levels simultaneously. The minimum in $^{91}\alpha$ between the two maxima to the high frequency side of the zirconium-90 peak is clearly associated with a local maximum in the zirconium-90 excitation rate. This maximum is not expected spectroscopically and may have been due to laser frequency jitter or poor S/N ratio considerations. Indeed we expect a maximum in $^{91}\alpha$ around this position. Nonetheless the demonstrated zirconium-91 selectivity is more than adequate, >10, using this simple pulsed oscillator though it is admittedly inferior to that obtained using the pulse amplified ring dye laser ($^{91}\alpha > 100$) [2].

SUMMARY AND CONCLUSIONS.

The measurements reported in this paper identify several suitable schemes for zirconium-91 AVLIS based on copper vapour laser pumped dye laser technology. Clearly an efficient route to zirconium-91 depleted material must involve selective removal of zirconium-91. If sufficient depletion is to be achieved in a single pass then at least the two lowest, preferably all three, spin-orbit split levels of the ground electronic configuration must be considered. These considerations together with the objective of a minimum number of separate laser frequencies limit the choice of first step intermediate levels to $z^3F_2^0$, $z^3F_3^0$, $z^3D_2^0$ and $z^3D_3^0$. The former has been rejected on the basis of the hyperfine structure for the transition $z^3F_2^0 \leftarrow a^3F_2$ reported in this study. We will consider the remaining three schemes in turn.

The intermediate level $z^3F_3^0$ has transitions to the ground state terms with suitable hyperfine structure. All seventeen hyperfine levels of the three ground configurations, with the exception of the F=13/2 sublevel of a^3F_4, can be excited by three laser frequencies chosen to the high frequency side of each band. From the $z^3F_3^0$ level excitation to a second intermediate level at

35209 cm^{-1} (λ_2=544.5 nm), identified in the two color resonance ionization work, followed by absorption of a photon of wavelength $\lambda < 546.6$ nm can result in ionization. Isotopically selective ionization via this scheme has been demonstrated using the SLM laser tuned to the transition $z^3F_3^0 \leftarrow a^3F_2$ at 593.7 nm followed by the absorption of two 544.5 nm photons.

The hyperfine structure of transitions from the ground state ^3F_J levels to $z^3D_3^0$ is suitable although selective removal of the F=11/2 substate of a^3F_3 and the F=13/2 and 1/2 level of a^3F_4 would not be achievable by high frequency edge excitation. From the $z^3D_3^0$ level numerous two photon resonance ionization schemes have been identified at wavelengths available from copper laser pumped dye lasers.

Schemes based upon the $z^3D_2^0$ level are less promising, principally as a result of the poor hyperfine structure for the $z^3D_2^0 \leftarrow a^3F_3$ transition coupled with the fact that the a^3F_4 state is not accessible.

We have not considered two photon ionization schemes in this study, although such schemes, particularly those based upon XeCl excimer pumped dye lasers, may be worthy of further consideration as the state of dye laser technology advances. The three photon schemes identifed here, particularly the two based upon the $z^3F_3^0$ and $z^3D_3^0$ levels deserve further attention. In particular cross-sections for transitions into and out of (ionization) the various resonant intermediate levels identified here are of interest.

The simple SLM oscillator used here will find wide application in various isotope enrichment and isotope determination experiments. This is a consequences of its low cost, ease of construction and narrow frequency, band-width limited, output. These properties are of particular relevance to zirconium AVLIS as multiple hyperfine levels of the ground state can be

depleted at single laser frequencies. This removes the need for the tumbling of hyperfine levels via RF fields suggested in earlier papers [2,13].

ACKNOWLEDGEMENTS.

We would like to thank Dr. John Alcock for the loan of the ring dye laser equipment and we would like to thank Dr. P. Pianorosa for generously communicating unpublished data to us.

References.

[1] J.L. Emmett, W.F. Krupke and J.I. Davis, IEEE J. Quantum Electron., QE-20, 591-602 (1984).

[2] M.R. Humphries, O.L. Bourne and P.A. Hackett, Chem. Phys. Lett., 118, 134-139 (1985).

[3] O.L. Bourne, M.R. Humphries, S.A. Mitchell and P.A. Hackett, Opt. Commun., 56 403-408 (1986).

[4] S. Büttgenbach, R. Dicke, H. Gebauer, R. Kuhnen and F. Träber, Z. Physik A286, 125-131 (1978).

[5] M.G. Littman, App. Opt., 23 4465-4468 (1984).

[6] O.L. Bourne and D.M. Rayner, Opt. Commun., submitted.

[7] R. Wallenstein and T.W. Hänsch, Appl. Opt., 13, 1625-1628 (1974).

[8] P.A. Hackett, M.R. Humphries, S.A. Mitchell and D.M. Rayner., J. Chem. Phys., 85 3194-3197 (1986).

[9] H.G. Kuhn, Atomic Spectra, 2nd Ed (Longman, London 1969) pp. 351.

[10] G. Chevalier, J-M. Gagné and P. Pianorosa, Opt. Commun., submitted.

[11] G. Chevalier, J-M. Gagné and P. Pianorosa, J. Opt. Soc. Am. B., submitted.

[12] C.E. Moore, Atomic Energy Levels, Nat. Bur. Stand. (US) Circ. 467, Vol. II, (1952).

[13] L.S. Goodman, O. Poulsen and W.J. Childs, Opt. Commun., 28, 309-310 (1979).

TABLE I. Optical transitions from the zirconium ground states accessible to copper vapour laser pumped dye lasers.

	Vacuum Wavelengths (nm)		
Excited State \ Ground State	a^3F_2	a^3F_3	a^3F_4
$z^3F_2^\circ$	613.6	635.9	...
$z^3F_3^\circ$	593.7	614.5	640.9
$z^3D_2^\circ$	561.4	579.9	...
$z^3D_3^\circ$	548.1	565.8	588.1

TABLE II. Hyperfine constants of zirconium-91.

Level Designation[a]	A (MHz)[b]	B (MHz)[b]
$(4d^2 5s5p)z^3F_2^\circ$	**-5.7±1.0**	**0.0**[c]
	(-3.5±0.8)	*(0.2±4.4)*
$(4d^2 5s5p)z^3F_3^\circ$	**-212.1±3.7**[d]	**8.7±18.1**[d]
	-209.4±4.5[e]	**31.5±23.6**[e]
	(-212.0±0.3)	*(-6.6±4.2)*
$(4d^2 5s5p)z^3D_2^\circ$	**-179.2±1.0**	**0.0**[c]
	(-179.1±0.6)	*(-1.9±3.0)*
$(4d^2 5s5p)z^3D_3^\circ$	**-301.78±0.033**	**-24.04±0.77**
	(-300.7±0.6)	*(-12.2±5.3)*

[a] Using the notation of Ref. 12.

[b] Values in parentheses are from Ref. 11.

[c] Set to zero for the least squares fit.

[d] Measured on the transition at 593.7 nm.

[e] Measured on the transition at 614.5 nm.

TABLE III. Isotope shifts in zirconium transitions.

Transition[a]	Vacuum Wavelength (nm)	Measured Shifts (MHz) $\Delta\nu$(90-91)[b]	$\Delta\nu$(90-92)[c]	$\Delta\nu$(90-94)[c]	$\Delta\nu$(90-96)[c]
$z^3F_2^\circ \leftarrow a^3F_2$	613.6	**107.7±0.19**	**213.2±2.3**	**379.2±3.2**	**503.0±6.0**
		(• • •)	*(210.5±5.1)*	*(372.6±6.7)*	*(499.9±7.7)*
$z^3F_3^\circ \leftarrow a^3F_2$	593.7	**88.4±6.2**	**214.0±3.8**	**380.5±5.8**	**498.3±7.5**
		(97.2±10.0)	*(221.3±5.7)*	*(386.5±7.6)*	*(511.8±8.8)*
$z^3F_3^\circ \leftarrow a^3F_3$	614.5	**89.8±7.1**	**232.7±5.3**	**389.4±8.3**	**508.5±10.7**
		(95.0±10.0)	*(226.0±7.7)*	*(390.9±10.2)*	*(521.2±11.9)*
$z^3D_2^\circ \leftarrow a^3F_3$	579.9	**102.1±4.5**	**215.6±2.9**	**392.3±0.9**	**520.9±5.8**
		(82.2±7.5)	*(227.5±3.8)*	*(398.2±4.8)*	*(530.9±5.8)*
$z^3D_3^\circ \leftarrow a^3F_4$	588.1	**102.3±0.21**	**242.8±6.5**	**414.9±6.6**	• • •
		(98.2±18.8)	*(240.5±5.2)*	*(418.0±7.2)*	*(530.1±8.2)*

[a] Using the notation of Ref. 12, for each transition the configuration of the lower level is $4d^25s^2$ and of the upper level is $4d^25s5p$.

[b] Values in parentheses are from Ref. 10.

[c] Values in parentheses are from Ref. 11.

Figures

1. Doppler-free fluorescence spectrum of the transition $z^3F_2^0 \leftarrow a^3F_2$ of ground state zirconium atoms at 613.6 nm. The even isotope peaks and five peaks arising from the hyperfine transition in ^{91}Zr are clearly resolved. Note that the hyperfine splitting is small for the upper state of this transition with the consequence that transitions from individual hyperfine levels of the ground state are removed from each other.
2. Doppler-free fluorescence spectrum of the transition $z^3F_3^0 \leftarrow a^3F_2$ of ground state zirconium atoms at 593.7 nm. The hyperfine transitions of zirconium-91 are labelled by the hyperfine quantum numbers of their lower levels. Note that for this transition the hyperfine splitting in the upper state is reasonably large with the consequence that transitions from individual hyperfine levels of the ground state lie within reasonable proximity to each other. Contrast this with the situation revealed in Figure 1.
3. Energy level diagram of the $z^3F_3^0 \leftarrow a^3F_2$ transition in zirconium, illustrating the isotope and hyperfine shifts. All the transitions listed in Table I exibit a similar structure. The $\Delta\lambda_{ij}$ are measured for peaks assigned in the spectra. The scale factor S, the excited state hyperfine constants A_e and B_e, and the isotope shift $\Delta 91$ are calculated by fitting the spectra to the known ground state hyperfine shifts Δg_i and known coefficients a_j and b_j (see Reference 9).
4. Energy level diagram of resonances in zirconium discovered by two color ionization. The transitions, all in vacuum wavelengths, from $z^3F_3^0$, $z^3D_3^0$ and $z^3D_2^0$ would be the second steps in possible photoionization schemes.

The long wavelength limit for the ionizing steps in such schemes are indicated for three of the resonances. The energy levels are indicated in cm^{-1}. Six of the resonances found from $z^3D_3^0$ lie at: a) 35860 cm^{-1}; b) 36331 cm^{-1} and 36344 cm^{-1}; c) 36916 cm^{-1}; and d) 36973 cm^{-1} and 36982 cm^{-1}.

5. Mass spectra obtained by 2 color resonance enhanced multiphoton ionization of zirconium atoms. The first laser wavelength was 593.7 nm to pump the $z^3F_3^0 \leftarrow a^3F_2$ resonance. A second laser tuned to a resonance from the $z^3F_3^0$ level at 544.5 nm provides 2 photons to ionize. For the upper panel (a) the first laser ran multimode; for the lower panel (b) it operated on a single longitudinal mode. The vertical scale of panel (b) has been expanded by a factor of two.

6. Frequency dependence of the isotopic selectivity, $^{91}\alpha$, (see text), is shown as the solid line in the upper panel. The points show the intensity of the zirconium-90 ionization peak and require the right hand ordinate. Smoothing the points by a 3 point average (weighted 1:2:1) yields the dashed line. Similar smoothing was applied to the ionization of the other isotopes. Selectivity was calculated from the smoothed data. The lower panel shows a stick representation (logarithmic ordinate) of the high resolution spectrum shown in Figure 2. The abscissa for the upper panel, originally SLM cavity N_2 pressure (see text), has been scaled by comparison of the positions of even isotope peaks with those in the lower panel.

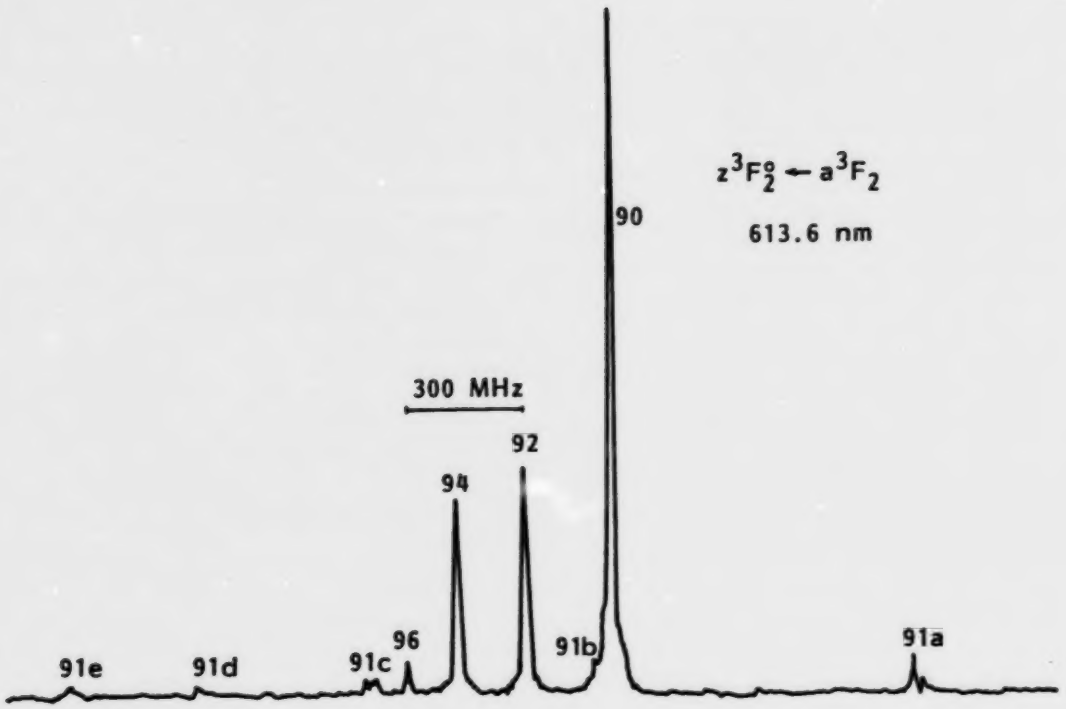

Fig. 1: P.A. Hackett et al.
Appl. Phys. B.

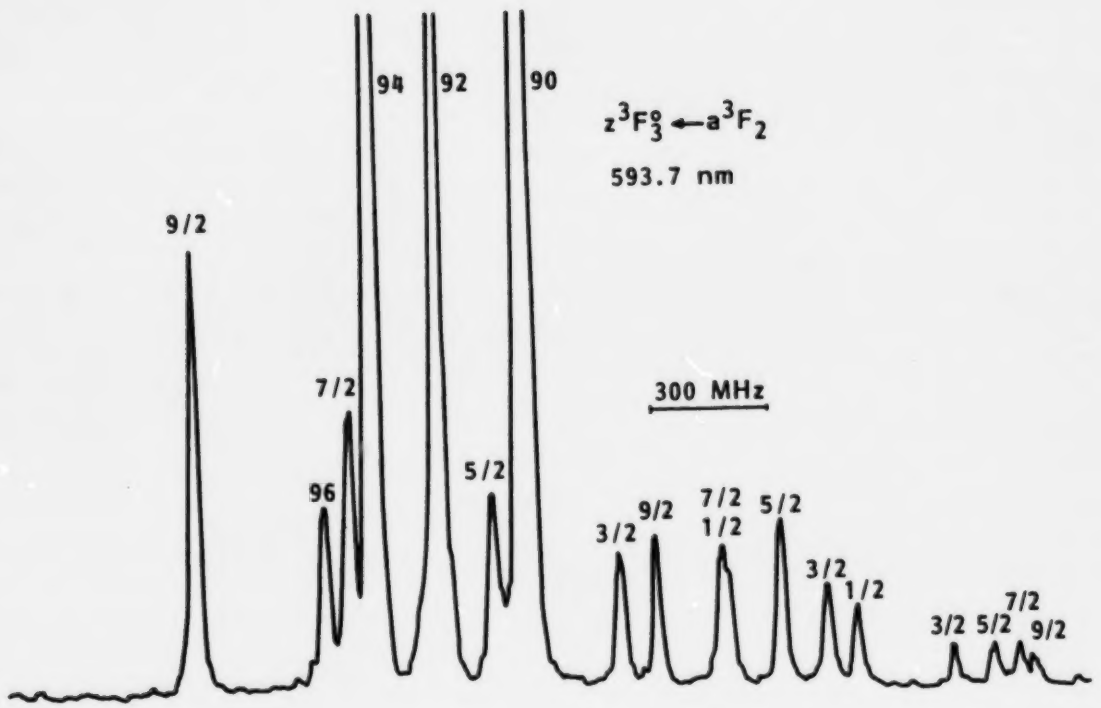

Fig. 2: P.A. Hackett et al.
Appl. Phys. B.

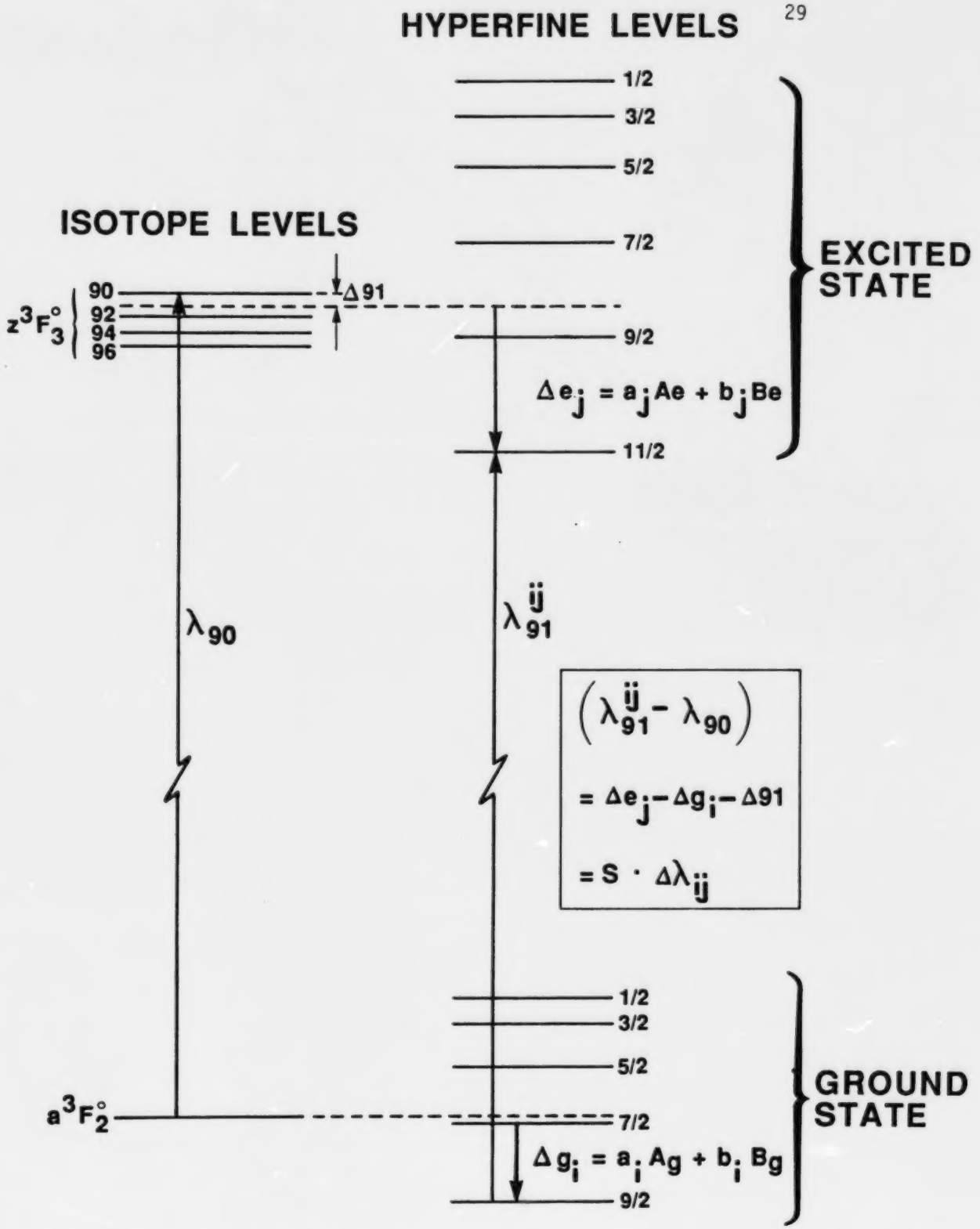

Fig. 3: P.A. Hackett et al.
Appl. Phys. B.

87-322

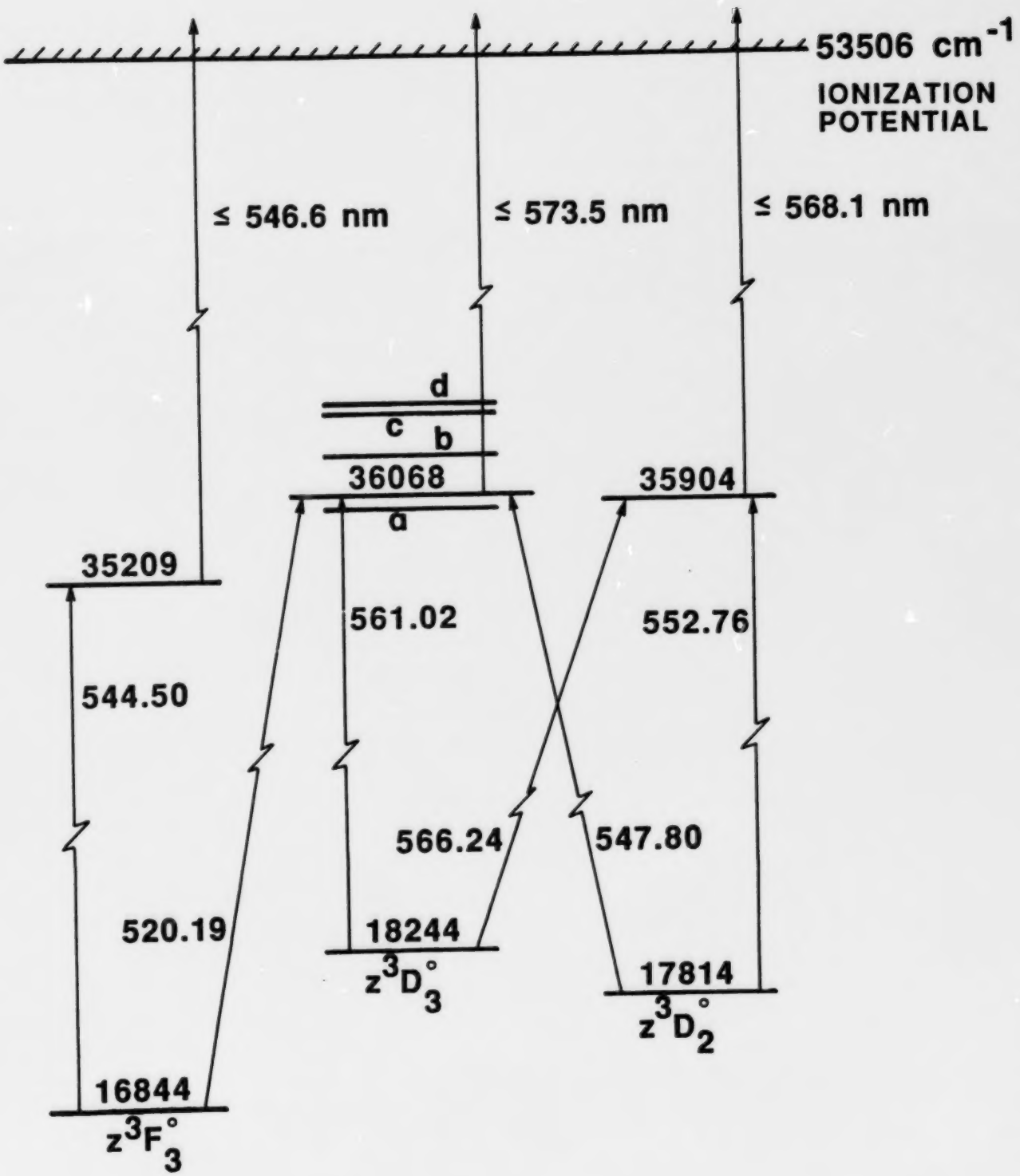

87-322

Fig. 4: P.A. Hackett et al. Appl. Phys. B.

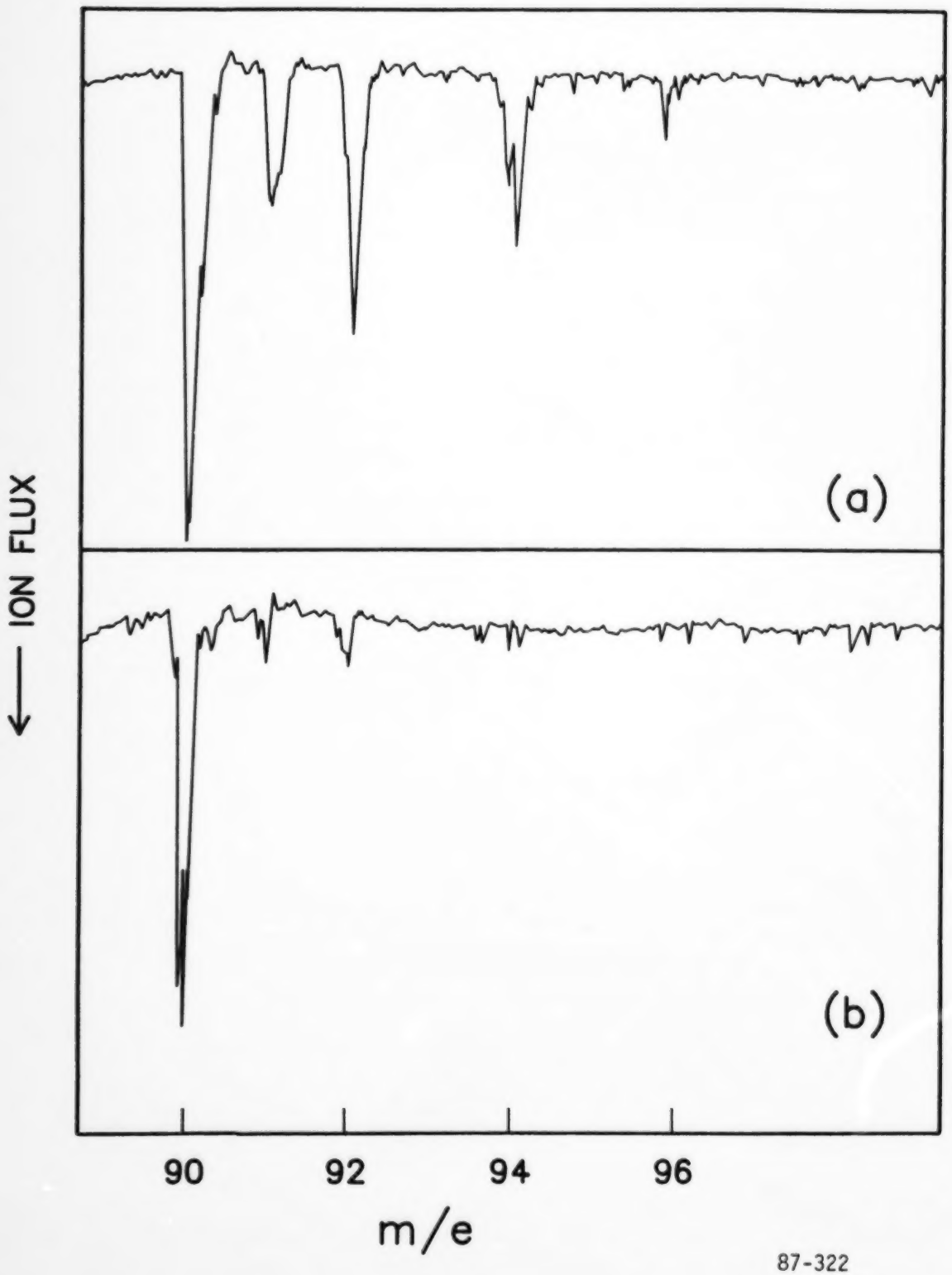

87-322

DF

Fig. 5: P.A. Hackett et al.
Appl. Phys. B.

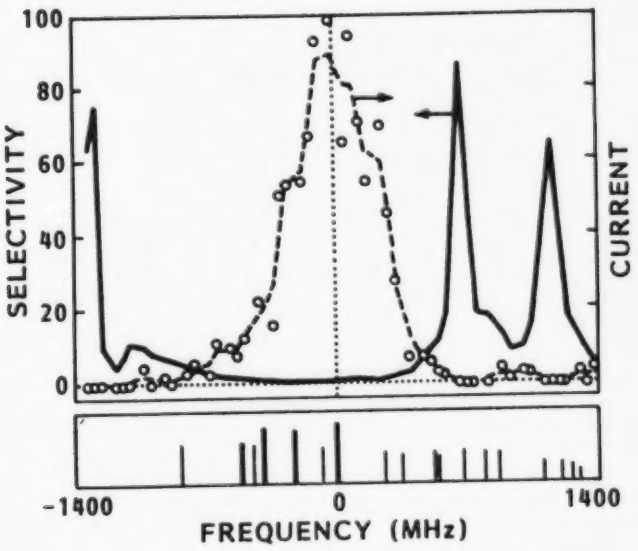

**Fig. 6: P.A. Hackett et al.
Appl. Phys. B.**